

# Klein-Nishina steps in the energy spectrum of galactic cosmic ray electrons

R. Schlickeiser\* and J. Ruppel\*\*

Institut für Theoretische Physik, Lehrstuhl IV: Weltraum- und Astrophysik, Ruhr-Universität Bochum, D-44780 Bochum, Germany

October 22, 2018

## ABSTRACT

The full Klein-Nishina cross section for the inverse Compton scattering interactions of electrons implies a significant reduction of the electron energy loss rate compared to the Thomson limit when the electron energy exceeds the critical Klein-Nishina energy  $E_K = \gamma_K m_e c^2 = 0.27 m_e^2 c^2 / (k_B T)$ , where  $T$  denotes the temperature of the photon graybody distribution. As a consequence the total radiative energy loss rate of single electrons exhibits sudden drops in the overall  $\dot{\gamma} \propto \gamma^2$ -dependence when the electron energy reaches the critical Klein-Nishina energy. The strength of the drop is proportional to the energy density of the photon radiation field. The diffuse galactic optical photon fields from stars of spectral type B and G-K lead to critical Klein-Nishina energies of 40 and 161 GeV, respectively. Associated with the drop in the loss rate are sudden increases (Klein-Nishina steps) in the equilibrium spectrum of cosmic ray electrons. Because the radiative loss rate of electrons is the main ingredient in any transport model of high-energy cosmic ray electrons, Klein-Nishina steps will modify any calculated electron equilibrium spectrum irrespective of the electron sources and spatial transport mode. To delineate most clearly the consequences of the Klein-Nishina drops in the radiative loss rate, we chose as illustrative example the simplest realistic model for cosmic ray electron dynamics in the Galaxy, consisting of the competition of radiative losses and secondary production by inelastic hadron-hadron collisions. We demonstrate that the spectral structure in the FERMI and H.E.S.S. data is well described and even the excess measured by ATIC might be explained by Klein-Nishina steps.

**Key words.** ISM: cosmic rays - Radiation mechanisms: non-thermal

## 1. Introduction

Recent measurements of the energy spectrum of local galactic cosmic ray electrons at energies above a few hundred GeV by the ATIC instrument<sup>1</sup> have reported a significant excess in the all-electron intensity that agrees at lower energies with the measurements of the PAMELA satellite experiment<sup>2</sup>, which also has observed a dramatic rise in the positron fraction starting at 10 GeV and extending up to 300 GeV. The significant ATIC excess has not been confirmed by the electron spectrum determinations with the FERMI satellite<sup>3</sup> and the H.E.S.S. air Cherenkov<sup>4</sup> experiments, although these measurements indicate some spectral structure deviating from a pure power law behaviour in the ATIC energy range. These observations have motivated a large number of interpretations, from possible signatures of dark matter annihilation (e.g.<sup>5</sup>) to nearby astrophysical electron sources.

Here we explain the ATIC excess by a classical effect which so far has not been discussed in this context: during their galactic propagation positrons and electrons with energies above 10 GeV are subject to synchrotron radiation losses in the galactic magnetic field of about  $3\mu\text{G}$  and inverse Compton radiation losses in galactic target photon fields listed in Table 1, including the universal microwave background radiation field, infrared photons and optical stellar photons. The diffuse galactic optical photons can be characterized by the superposition of two graybody distributions (see the discussion in section 2.3 of<sup>6</sup>):

1) photons from stars of spectral type G-K with energy density  $W_G = 0.3 \text{ eV cm}^{-3}$  and temperature  $T_G = 5000 \text{ K}$ , cor-

responding to a mean photon energy  $\langle \epsilon \rangle_G = 2.7 k_B T_G = 2.327 \cdot 10^{-4} T_G = 1.16 \text{ eV}$ ;

2) photons from stars of spectral type B with energy density  $W_B = 0.09 \text{ eV cm}^{-3}$  and temperature  $T_B = 20000 \text{ K}$ , corresponding to a mean photon energy  $\langle \epsilon \rangle_B = 2.7 k_B T_G = 2.327 \cdot 10^{-4} T_B = 4.65 \text{ eV}$ .

For electron Lorentz factors  $\gamma$  much smaller than the critical Klein-Nishina Lorentz factor  $\gamma_K = 0.27 m_e c^2 / k_B T = 1.58 \cdot 10^9 / T(\text{K})$  (see Eq. (3) below), the inverse Compton scattering cross section of a single electron can be well approximated by the Thomson cross section resulting in the standard energy loss rate of single electrons  $\dot{\gamma} = -4c\sigma_T W \gamma^2 / (3m_e c^2)$ , where  $\sigma_T = 6.65 \cdot 10^{-25} \text{ cm}^2$  denotes the Thomson cross section and  $c$  the speed of light. However, for Lorentz factors  $\gamma \geq \gamma_{KN}$  the full Klein-Nishina cross section has to be used<sup>7,8,9,10</sup> resulting in a significant reduction of the inverse Compton loss rate. For the two graybody optical photon distributions the respective critical Klein-Nishina Lorentz factors are  $\gamma_{KN,G} = 3.2 \cdot 10^5$ , corresponding to an electron energy of  $E_{KN,G} = 161 \text{ GeV}$ , and  $\gamma_{KN,B} = 7.9 \cdot 10^4$ , corresponding to an electron energy of  $E_{KN,B} = 40 \text{ GeV}$ . We will demonstrate that this Klein-Nishina reduction of the inverse Compton energy loss rate leads to Klein-Nishina steps in the cosmic ray electron equilibrium spectrum which describes the observed FERMI and H.E.S.S. data well. In Sect. 2 we determine the galactic synchrotron and inverse Compton energy loss rates in the full Klein-Nishina case. For the illustrative example of a purely secondary origin of galactic electrons we show in Sect. 3 the resulting Klein-Nishina steps in comparison with the recent electron spectrum observations.

\* e-mail: rsch@tp4.ruhr-uni-bochum.de

\*\* e-mail: jr@tp4.ruhr-uni-bochum.de

**Table 1.** Electromagnetic graybody radiation fields in the local interstellar medium

i	comment	$T_i / \text{K}$	$W_i / \frac{\text{eV}}{\text{cm}^3}$	$\gamma_{K,i}$	$E_{K,i} / \text{GeV}$
1	spectral type B	20000	0.09	$7.9 \cdot 10^4$	40
2	spectral type G - K	5000	0.3	$3.2 \cdot 10^5$	161
3	infrared	20	0.4	$7.9 \cdot 10^7$	$4.0 \cdot 10^4$
4	microwave	2.7	0.25	$5.9 \cdot 10^8$	$3.0 \cdot 10^5$

## 2. Synchrotron and inverse Compton energy loss rates

The synchrotron energy loss rate of a single electron in a large-scale random magnetic field of constant strength  $B$  is<sup>11</sup>

$$|\dot{\gamma}|_S = \frac{4\sigma_{TC}}{3m_e c^2} U_B \gamma^2, \quad (1)$$

where  $U_B = B^2/8\pi = 0.22b_3^2 \text{ eV cm}^{-3}$  if we scale the galactic magnetic field strength as  $B = 3b_3 \mu\text{G}$ .

In the Appendix we approximately calculate the inverse Compton energy loss rate of a single electron in one graybody photon field as

$$|\dot{\gamma}|_C \approx \frac{4\sigma_{TC} W}{3m_e c^2} \frac{\gamma_K^2 \gamma^2}{\gamma_K^2 + \gamma^2}, \quad (2)$$

where the critical Klein-Nishina Lorentz factor is given by

$$\gamma_K \equiv \frac{3\sqrt{5} m_e c^2}{8\pi k_B T} = \frac{0.53 m_e c^2}{k_B T}. \quad (3)$$

For small electron Lorentz factors  $\gamma \ll \gamma_K$  the general inverse Compton energy loss rate (2) reduces to the Thomson limit

$$|\dot{\gamma}|_C (\gamma \ll \gamma_K) \approx \frac{4\sigma_{TC} W}{3\pi^4 m_e c^2} \gamma^2, \quad (4)$$

whereas for large electron Lorentz factors  $\gamma \gg \gamma_K$  we obtain the energy-independent extreme Klein Nishina limit

$$|\dot{\gamma}|_C (\gamma \gg \gamma_{KN}) \approx \frac{4\sigma_{TC} W}{3m_e c^2} \gamma_K^2. \quad (5)$$

The total radiative (synchrotron and inverse Compton) energy loss rate of a single electron is given by the sum of rate (1) and rates (2) for the four diffuse galactic radiation fields listed in Table 1, yielding

$$|\dot{\gamma}|_R = \frac{4\sigma_{TC} U_B \gamma^2}{3m_e c^2} \left[ 1 + \sum_{i=1}^4 \frac{W_i}{U_B} \frac{\gamma_{K,i}^2}{\gamma^2 + \gamma_{K,i}^2} \right]. \quad (6)$$

In Figure 1 we show the resulting radiative energy loss rate for the local galactic magnetic field and photon energy densities for relativistic electrons with energies between 1 and  $10^7$  GeV. One clearly notices the four sudden drops whenever the electron energy reaches each of the critical Klein-Nishina energies. The strength of the drop is proportional to the energy density of the photon field. For electron Lorentz factor below the smallest critical Klein-Nishina Lorentz factor all four graybody photon fields plus the magnetic field energy density contribute to the loss rate. Once the electron Lorentz factor has exceeded the critical Klein-Nishina Lorentz factor of a particular photon field, this photon field no longer contributes to the radiative loss rate due to the much reduced inverse Compton loss rate in the Klein-Nishina limit. At Lorentz factors above the maximum critical Lorentz factor from the microwave background photons  $\gamma_{k,4} = 5.9 \cdot 10^8$  only synchrotron losses contribute to the radiative loss rate.

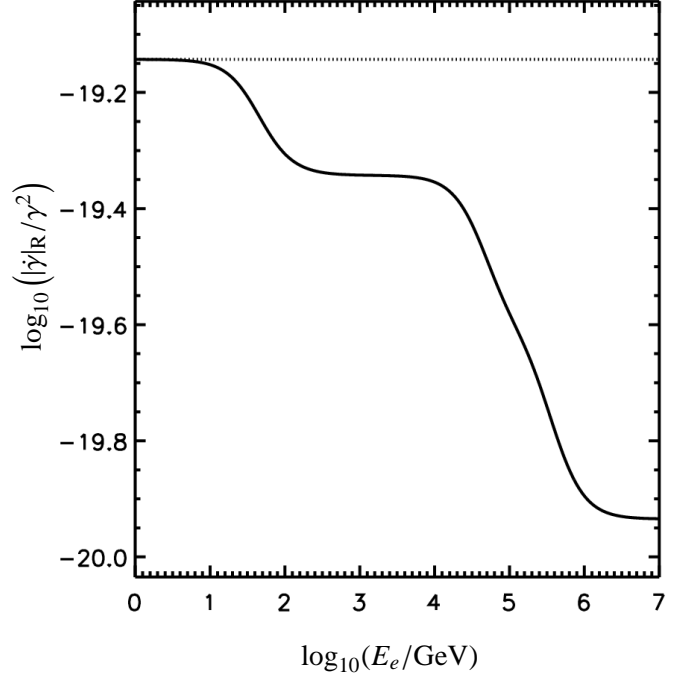


**Fig. 1.** The energy loss of relativistic electrons – as given by equation (6) – as a function of the electron energy in GeV. The solid line shows four drops related to the critical Klein-Nishina energies, whereas the dotted line illustrates synchrotron and inverse Compton losses in the Thomson limit.

## 3. Klein-Nishina steps in the electron equilibrium spectrum

In this section we calculate the equilibrium spectrum of galactic cosmic ray electrons above 10 GeV taking into account the modified radiative loss rate (6), as well as non-thermal bremsstrahlung, adiabatic deceleration losses in a possible galactic wind with the velocity  $v_{gw}$  and Coulomb and ionization losses<sup>15</sup>. Because the radiative loss rate of electrons is the main ingredient in any transport model of high-energy cosmic ray electrons, Klein-Nishina steps will modify any calculated electron equilibrium spectrum irrespective of the electron sources and spatial transport mode. To delineate most clearly the consequences of the Klein-Nishina drops in the radiative loss rate, we chose as illustrative example the simplest realistic model for cosmic ray electron dynamics in the Galaxy. Extensions to more sophisticated models of cosmic ray electron dynamics (influence of localized point sources, spatial diffusion, convection and distributed reacceleration), where the consequences of the modified inverse Compton losses also occur, are the subject of future work.

At electron energies above 10 GeV the electron's radiative loss time  $\tau_R = \gamma/|\dot{\gamma}_R| \propto \gamma^{-1}$  is so short that the Galaxy behaves as a thick target or fractional calorimeter<sup>14,15</sup> for the electrons. The equilibrium energy spectrum of cosmic ray electrons  $N(\gamma)$  then results from the balance of electron production, expressed as injection spectrum  $Q(\gamma)$ , and radiative energy losses from the solution of the balance equation

$$\frac{d}{d\gamma} [|\dot{\gamma}_R(\gamma)|N(\gamma)] + Q(\gamma) = 0, \quad (7)$$

implying

$$N(\gamma) = |\dot{\gamma}_R(\gamma)|^{-1} \int_{\gamma}^{\infty} dy Q(y). \quad (8)$$

Moreover, we assume here that all electrons are secondaries resulting from inelastic hadron-hadron collisions of primary cosmic ray hadrons with interstellar gas atoms and molecules during their confinement in the Galaxy. It is well established<sup>16,17</sup> that secondary production accounts for the major part of the observed galactic cosmic ray electrons at relativistic energies. The locally measured hadron spectrum<sup>18</sup> at energies below  $4.4 \cdot 10^{15}$  GeV is a power law  $\propto \gamma_h^{-s}$ , with spectral index  $s = 2.74$ . Using the hadron-hadron cross section templates<sup>19</sup> the resulting electron injection spectrum at energies above 10 GeV,  $Q(\gamma) = Q_0 \gamma^{-s}$ , then follows a power law with the hadron spectral index  $s$ . With this injection spectrum and the radiative energy loss rate (6) the equilibrium spectrum (8) becomes

$$\begin{aligned} N(\gamma) &= \frac{Q_0 \gamma^{1-s}}{(s-1) |\dot{\gamma}_R(\gamma)|} \\ &= \frac{3m_e c^2 Q_0 \gamma^{-s-1}}{4(s-1) \sigma_T c U_B} \left[ 1 + \sum_{i=1}^4 \frac{W_i}{U_B} \frac{\gamma_{K,i}^2}{\gamma^2 + \gamma_{K,i}^2} \right]^{-1} \end{aligned} \quad (9)$$

which is shown in Figure 3 in comparison with the observed energy spectrum of galactic cosmic ray electrons. It can be seen that the spectral shape of the H.E.S.S. and FERMI data is well fitted. In Figure 2 the Klein-Nishina steps are clearly visible.

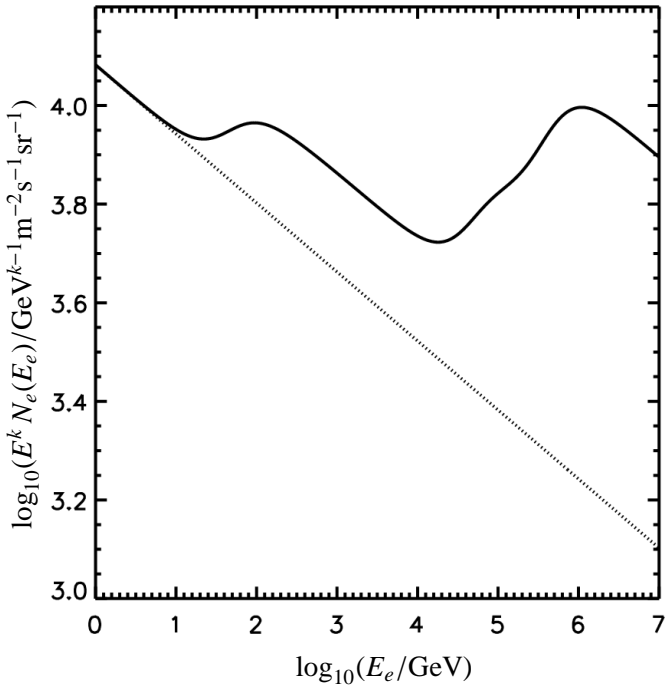


**Fig. 2.** The equilibrium spectrum of cosmic ray electrons as a function of the electron energy in GeV. The solid line represents the electron spectrum with Klein-Nishina corrections, the dotted line shows the spectrum in the Thomson limit. The comparison of the shapes clearly illustrates the impact of the Klein-Nishina corrections.

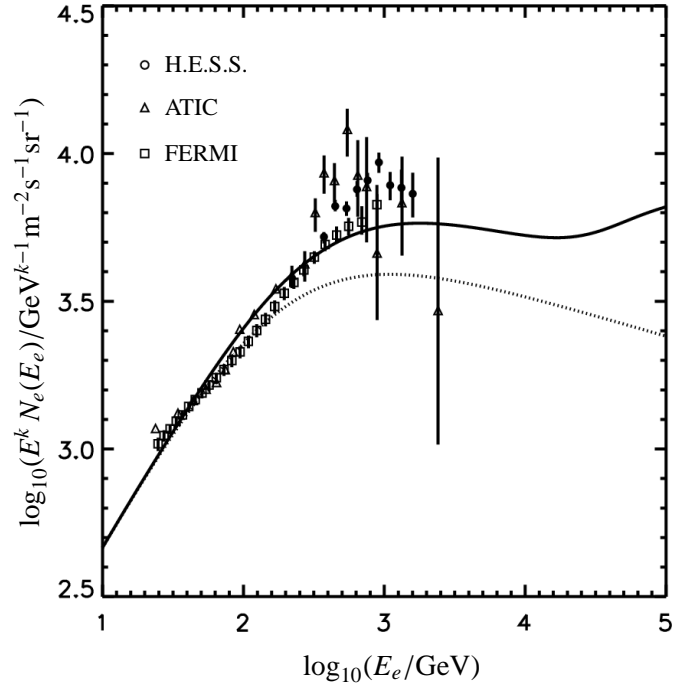


**Fig. 3.** The equilibrium spectrum of cosmic ray electrons as a function of the electron energy in GeV compared to observational data by H.E.S.S., ATIC and FERMI. Again, the solid line represents the electron spectrum with Klein-Nishina corrections, the dotted line shows the spectrum in the Thomson limit. Whereas here, the full energy losses are taken into account. The values of the parameters are:  $B = 3 \mu\text{G}$ ,  $n_H = 0.3 \text{ cm}^{-3}$ , Degree of ionisation: 0.2,  $k = 3.6$ ,  $\text{div}(v_{gw}) = 10^{-13.13} \text{ s}^{-1}$

#### 4. Summary and conclusions

The full Klein-Nishina cross section for the inverse Compton scattering interactions of electrons implies a significant reduction of the electron energy loss rate compared to the Thomson limit when the electron energy exceeds the critical Klein-Nishina energy  $E_K = \gamma_K m_e c^2 = 0.27 m_e^2 c^2 / (k_B T)$ , where  $T$  denotes the temperature of the photon graybody distribution. As a consequence the total radiative energy loss rate of single electrons exhibits sudden drops in the overall  $\dot{\gamma} \propto \gamma^2$ -dependence when the electron energy reaches the critical Klein-Nishina energy. The strength of the drop is proportional to the energy density of the photon radiation field. The diffuse galactic optical photon fields from stars of spectral type B and G-K lead to critical Klein-Nishina energies of 40 and 161 GeV, respectively. Associated with the drop in the loss rate are sudden increases (Klein-Nishina steps) in the equilibrium spectrum of cosmic ray electrons (see Figure 2). Because the radiative loss rate of electrons is the main ingredient in any transport model of high-energy cosmic ray electrons, Klein-Nishina steps will modify any calculated electron equilibrium spectrum irrespective of the electron sources and spatial transport mode. To delineate most clearly the consequences of the Klein-Nishina drops in the radiative loss rate, we chose as illustrative example the simplest realistic model for cosmic ray electron dynamics in the Galaxy, consisting of the competition of radiative losses and secondary production by inelastic hadron-hadron collisions. We demonstrate that the spectral structure in the FERMI and H.E.S.S. data is well described and even the excess measured by ATIC might be explained by Klein-Nishina steps.

After completing this work we noticed the recent preprint by Stawarz, Petrosian and Blandford (2009) who also explain the recently measured galactic electron spectrum by the Klein-Nishina suppression of the inverse Compton energy loss of relativistic electrons in an optical photon field with an energy density of  $3 \text{ eV cm}^{-3}$ .

*Acknowledgements.* This work was partially supported by the German Ministry for Education and Research (BMBF) through Verbundforschung Astroteilchenphysik grant 05 A08PC1 and the Deutsche Forschungsgemeinschaft through grant Schl 201/20-1.

## References

- J. Chang et al., Nature 456, 362 (2008)  
 O. Adriani et al., Nature 458, 607 (2009)  
 A.A. Abdo, et al., PRL 102, 181101 (2009)  
 F. Aharonian, et al., PRL 101, 261104 (2008)  
 M. Sipet, D. Hooper, astro-ph 904.2398 (2009)  
 R. Schlickeiser, Cosmic Ray Astrophysics (Springer, Heidelberg, 2002)  
 F. C. Jones, Phys. Rev. 137, B1306 (1965)  
 G. R. Blumenthal, R. J. Gould, Rev. Modern Phys. 42, 237 (1970)  
 R. Schlickeiser, ApJ 233, 294 (1979)  
 T. Prince, R. Schlickeiser, Proc. 16th International Cosmic Ray Conference, Vol. 1, 155 (1979)  
 A. Crusius, R. Schlickeiser, Astr. Ap. 196, 327 (1988)  
 O. Petruk, Astr. Ap. 499, 643 (2009)  
 R. Schlickeiser, MNRAS, in press (2009)  
 H. J. Völk, Astr. Ap. 218, 983 (1989)  
 M. Pohl, Astr. Ap. 270, 91 (1993)  
 A. M. Lionetto, M. Morselli, A., V. Zdravkovic, J. Cosmol. Astro-Part. Phys. 9, 10 (2005)  
 T. Delahaye, R. Lineros, F. Donato, N. Fornengo, J. Lavalle, P. Salati, R. Taillet, Astr. Ap. 501, 821 (2009)  
 T. Antoni, et al., ApJ 612, 914 (2004)  
 S.R. Kelner, F. A. Aharonian, V. V. Bugayov, Phys. Rev. D 74, 034018 (2006)

## Appendix A: Inverse Compton energy loss rate in graybody photon distributions

The inverse Compton power of a single electron in a general target photon field  $n(\epsilon)$  is (Ch. 4.2 in<sup>6</sup>)

$$p_C(\epsilon_s, \gamma) = c \int_0^\infty d\epsilon n(\epsilon) \epsilon_s \sigma(\epsilon_s, \epsilon, \gamma), \quad (\text{A.1})$$

where  $\epsilon_s$  denotes the scattered photon energy. The differential Klein-Nishina cross section<sup>8</sup> is given by

$$\sigma(\epsilon_s, \epsilon, \gamma) = \frac{3\sigma_T}{4\epsilon\gamma^2} G(q, \Gamma) \quad (\text{A.2})$$

with

$$G(q, \Gamma) = G_0(q) + \frac{\Gamma^2 q^2 (1-q)}{2(1+\Gamma q)} \quad (\text{A.3})$$

where  $G_0(q) = 2q \ln q + (1+2q)(1-q)$

and

$$\Gamma = \frac{4\epsilon\gamma}{mc^2}, \quad q = \frac{\epsilon_s}{\Gamma\gamma mc^2 - \epsilon_s}. \quad (\text{A.4})$$

By integrating over all kinematically allowed scattered photon energies we find for the inverse Compton energy loss rate of a single electron

$$\begin{aligned} |\dot{\gamma}|_C &= \frac{1}{mc^2} \int_0^{\epsilon_{s,\max}} d\epsilon_s p_C(\epsilon_s, \gamma) \\ &= \frac{3c\sigma_T}{4mc^2\gamma^2} \int_0^\infty d\epsilon \epsilon^{-1} n(\epsilon) \int_0^{\epsilon_{s,\max}} d\epsilon_s \epsilon_s G(q, \Gamma), \end{aligned} \quad (\text{A.5})$$

where  $\epsilon_{s,\max} = \Gamma\gamma mc^2/(\Gamma+1)$  corresponds to  $q = 1$ . Using  $q$  as integration variable instead of  $\epsilon_s$  results in

$$\begin{aligned} |\dot{\gamma}|_C &= \frac{12c\sigma_T}{m_e c^2} \gamma^2 \int_0^\infty d\epsilon \epsilon n(\epsilon) J(\Gamma) \\ &\text{with } J(\Gamma) = \int_0^1 dq \frac{qG(q, \Gamma)}{(1+\Gamma q)^3}. \end{aligned} \quad (\text{A.6})$$

For the graybody photon distribution

$$n_G(\epsilon) = \frac{15W}{\pi^4 (k_B T)^4} \frac{\epsilon^2}{\exp[\epsilon/k_B T] - 1} \quad (\text{A.7})$$

the inverse Compton energy loss rate then is

$$\begin{aligned} |\dot{\gamma}|_C &= \frac{20c\sigma_T W}{\pi^4 m_e c^2} \gamma^2 I(\gamma, T) \\ &\text{with } I(\gamma, T) = 9(k_B T)^{-4} \int_0^\infty d\epsilon \frac{\epsilon^3}{\exp[\epsilon/k_B T] - 1} J(\Gamma). \end{aligned} \quad (\text{A.8})$$

Jones<sup>7</sup> already noted that the double integral  $I(\gamma, T)$  cannot be solved exactly, so that approximations (see e.g.<sup>12</sup>) are required. It has been noted<sup>13</sup> that the integral  $J(\Gamma)$  is reasonably well approximated by

$$J(\Gamma) = \int_0^1 dq \frac{qG(q, \Gamma)}{(1+\Gamma q)^3} \simeq \frac{1}{9+2\Gamma^2}, \quad (\text{A.9})$$

so that the double integral in Eq. (A.8) becomes

$$I(\gamma, T) = (k_B T)^{-4} \int_0^\infty d\epsilon \frac{\epsilon^3}{\exp[\epsilon/k_B T] - 1} \frac{1}{1 + \frac{32\gamma^2 \epsilon^2}{9m_e^2 c^4}}. \quad (\text{A.10})$$

With the substitution  $x = \epsilon/k_B T$  we find

$$I(A) = \int_0^\infty dx \frac{x^3}{1 + \frac{x^2}{A^2}} \frac{1}{e^x - 1}, \quad (\text{A.11})$$

where

$$A = \frac{3m_e c^2}{\sqrt{32}} k_B T \gamma. \quad (\text{A.12})$$

The series

$$\frac{1}{1 + \frac{x^2}{A^2}} = \sum_{k=1}^\infty (-1)^{k-1} \frac{x^{2(k-1)}}{A^{2(k-1)}}$$

leads to

$$I(A) = \sum_{k=1}^\infty (-1)^{k-1} \frac{\Gamma[2k+2] \zeta[2k+2]}{A^{2(k-1)}}, \quad (\text{A.13})$$

which, for  $A \geq 1$  to lowest order in  $A^{-2}$ , yields

$$I(A \geq 1) \simeq \Gamma[4] \zeta[4] = \frac{\pi^4}{15}. \quad (\text{A.14})$$

For  $A < 1$  we approximate the integral (A.11) by

$$\begin{aligned} I(A < 1) &\simeq \int_0^A dx \frac{x^3}{e^x - 1} + A^2 \int_A^\infty dx \frac{x}{e^x - 1} \\ &\simeq A^2 \int_0^\infty dx \frac{x}{e^x - 1} + \int_0^A dx x^2 - A^3 \\ &= \frac{\pi^2 A^2}{6} - \frac{2A^3}{3} \simeq \frac{\pi^2 A^2}{6} \end{aligned} \quad (\text{A.15})$$

We combine the two expansions (A.14) and (A.15) to

$$I(A) \simeq \frac{\pi^4}{15} \frac{1}{1 + \frac{2\pi^2}{5A^2}} \quad (\text{A.16})$$

valid at all values of  $A$ . The approximation (A.16) can be written as

$$I(A) \simeq \frac{\pi^4}{15} \frac{1}{1 + \left(\frac{\gamma}{\gamma_K}\right)^2}, \quad (\text{A.17})$$

where we introduce the critical Klein-Nishina Lorentz factor

$$\gamma_K \equiv \frac{3\sqrt{5}}{8\pi} \frac{m_e c^2}{k_B T} = \frac{0.27 m_e c^2}{k_B T}. \quad (\text{A.18})$$

Using this approximation in Eq. (A.8) readily yields the inverse Compton loss rate (2).

This figure "figure\_1.png" is available in "png" format from:

<http://arxiv.org/ps/0908.2183v1>

This figure "figure\_2.png" is available in "png" format from:

<http://arxiv.org/ps/0908.2183v1>

This figure "figure\_3.png" is available in "png" format from:

<http://arxiv.org/ps/0908.2183v1>